



## Article

# Climate Sensitivity of the Arid Scrublands on the Tibetan Plateau Mediated by Plant Nutrient Traits and Soil Nutrient Availability

Ben Chen <sup>1,2,†</sup>, Hui Chen <sup>1,†</sup>, Meng Li <sup>3</sup>, Sebastian Fiedler <sup>4</sup>, Mihai Ciprian Mărgărint <sup>5</sup>, Arkadiusz Nowak <sup>6,7</sup>, Karsten Wesche <sup>8,9,10</sup>, Britta Tietjen <sup>11,12</sup> and Jianshuang Wu <sup>2,5,\*</sup>

- <sup>1</sup> Hebei Key Laboratory of Environmental Change and Ecological Construction, Hebei Technology Innovation Center for Remote Sensing Identification of Environmental Change, School of Geographical Sciences, Hebei Normal University, Shijiazhuang 050024, China
  - <sup>2</sup> Institute of Environment and Sustainable Development in Agriculture, Chinese Academy of Agricultural Sciences, Beijing 100081, China
  - <sup>3</sup> School of Geographic Sciences, Nantong University, Nantong 226007, China
  - <sup>4</sup> Department of Ecosystem Modelling, Bűsgen-Institute, Universitat Göttingen, 37077 Göttingen, Germany
  - <sup>5</sup> Department of Geography, Geography and Geology Faculty, Alexandru Ioan Cuza University of Iași, 700505-RO Iași, Romania
  - <sup>6</sup> Botanical Garden Center for Biological Diversity Conservation in Powsin, Polish Academy of Sciences, 02-973 Warsaw, Poland
  - <sup>7</sup> Department of Botany and Nature Conservation, University of Warmia and Mazury in Olsztyn, Plac Łódzki 1, 10-727 Olsztyn, Poland
  - <sup>8</sup> Department of Botany, Senckenberg Museum of Natural History Görlitz, 02826 Görlitz, Germany
  - <sup>9</sup> International Institute (IHI) Zittau, Technische Universitat Dresden, 02763 Zittau, Germany
  - <sup>10</sup> German Centre for Integrative Biodiversity Research (iDiv) Halle-Jena-Leipzig, 04103 Leipzig, Germany
  - <sup>11</sup> Institute of Biology, Theoretical Ecology, Freie Universitat Berlin, 14195 Berlin, Germany
  - <sup>12</sup> Berlin-Brandenburg Institute of Advanced Biodiversity Research, 14195 Berlin, Germany
- \* Correspondence: wujianshuang@caas.cn  
† These authors contributed equally to this work.



**Citation:** Chen, B.; Chen, H.; Li, M.; Fiedler, S.; Mărgărint, M.C.; Nowak, A.; Wesche, K.; Tietjen, B.; Wu, J.

Climate Sensitivity of the Arid Scrublands on the Tibetan Plateau Mediated by Plant Nutrient Traits and Soil Nutrient Availability. *Remote Sens.* **2022**, *14*, 4601. <https://doi.org/10.3390/rs14184601>

Academic Editor: Xander Wang

Received: 25 July 2022

Accepted: 6 September 2022

Published: 15 September 2022

**Publisher's Note:** MDPI stays neutral with regard to jurisdictional claims in published maps and institutional affiliations.



**Copyright:** © 2022 by the authors. Licensee MDPI, Basel, Switzerland. This article is an open access article distributed under the terms and conditions of the Creative Commons Attribution (CC BY) license (<https://creativecommons.org/licenses/by/4.0/>).

## Highlights:

### What are the main findings?

- Principal component regressions revealed the climate sensitivity of Tibetan arid desert scrubs.
- Plant nutrient traits and soil nutrient availability regulate desert scrubs' climate sensitivity.

### What is the implication of the main finding?

- Scrubs' sensitivity to temperature is mainly regulated by the nitrogen contents of soils and leaves.
- Scrubs' sensitivity to precipitation is affected by the leaf carbon content of dominant species.
- Neither soil nor plant nutritional properties alone can well explain scrubs' sensitivity to droughts.

**Abstract:** Climate models predict the further intensification of global warming in the future. Drylands, as one of the most fragile ecosystems, are vulnerable to changes in temperature, precipitation, and drought extremes. However, it is still unclear how plant traits interact with soil properties to regulate drylands' responses to seasonal and interannual climate change. The vegetation sensitivity index (VSI) of desert scrubs in the Qaidam Basin (NE Tibetan Plateau) was assessed by summarizing the relative contributions of temperature ( $S_{GST}$ ), precipitation ( $S_{GSP}$ ), and drought (temperature vegetation dryness index,  $S_{TVDI}$ ) to the dynamics of the normalized difference vegetation index (NDVI) during plant growing months yearly from 2000 to 2015. Nutrient contents, including carbon, nitrogen, phosphorus, and potassium in topsoils and leaves of plants, were measured for seven types of desert scrub communities at 22 sites in the summer of 2016. Multiple linear and structural equation models were used to reveal how leaf and soil nutrient regimes affect desert scrubs' sensitivity to climate variability. The results showed that total soil nitrogen (STN) and leaf carbon content (LC), respectively, explained 25.9% and 17.0% of the VSI variance across different scrub communities. Structural equation modeling (SEM) revealed that STN and total soil potassium (STK) mediated desert scrub's

VSI indirectly via  $S_{GST}$  (with standardized path strength of  $-0.35$  and  $+0.32$ , respectively) while LC indirectly via  $S_{GST}$  and  $S_{GSP}$  (with standardized path strength of  $-0.31$  and  $-0.19$ , respectively). Neither soil nor leaf nutrient contents alone could explain the VSI variance across different sites, except for the indirect influences of STN and STK via  $S_{TVDI}$  ( $-0.18$  and  $0.16$ , respectively). Overall, this study disentangled the relative importance of plant nutrient traits and soil nutrient availability in mediating the climatic sensitivity of desert scrubs in the Tibetan Plateau. Integrating soil nutrient availability with plant functional traits together is recommended to better understand the mechanisms behind dryland dynamics under global climate change.

**Keywords:** climate change; dryland ecosystem; leaf nutrient traits; Qaidam Basin; soil nutrient availability; vegetation sensitivity index

## 1. Introduction

Drylands cover approximately 41% of the Earth's land surface [1] and support more than 38% of the global population [2], although they are sparsely vegetated and with limited productivity. Recently, drylands have been degraded due to ongoing climate change and intensifying human disturbance [3,4]. For example, increased droughts mainly caused by warming are predicted to accelerate the degradation of the Mediterranean drylands under human overexploitation [5]. More than 75% of drylands in developing countries are also likely to expand due to further global warming [6]. Consequently, poverty alleviation will become more challenging in arid undeveloped countries [7]. Therefore, a better understanding of how drylands respond to changes in climate and other potential regulators is urgently needed.

Climate change drives dryland dynamics across different spatial scales, including warming, shifting precipitation regimes, and intensifying droughts. Warming can limit plant growth and survival via increasing evapotranspiration and intensifying water deficit in soils [8,9]. Experimental studies have reported that increased precipitation can improve nutrient availability and facilitate plant growth, development, and reproduction in drylands via enhancing moisture content in topsoils and vice versa [10,11]. Meanwhile, remote-sensing-related technologies help monitor large-scale vegetation dynamics [12]. However, current studies on ecosystem responses to climate change are mainly based on average climate states but usually ignore the effects of climate variability and extremes [13].

Recently, Seddon et al. [14] have proposed a framework to assess the vegetation sensitivity index (VSI) to short-term variability in temperature, precipitation, and radiation (cloud mask) from a global perspective. Such an algorithm has been increasingly applied to reveal the relative importance of different climatic variables in driving the dynamics in vegetation coverage, productivity, and phenology within and across various ecosystems [15–18]. For example, Li et al. [15] assessed the variability of VSI with altitude gradient in alpine grasslands on the Tibetan Plateau and found that vegetation in higher altitude regions is more sensitive to climate variability than that in lower altitudes. In another study, Yuan et al. [18] found that vegetation in Central Asia was more sensitive to climate variability in spring than other three seasons. These studies have mapped the differential spatiotemporal patterns of alpine and arid vegetation in response to climate variability and greatly enhanced our understanding of the vegetation–climate relationship. However, they failed to provide mechanistic explanations for these patterns from the perspective of plant and soil nutrient properties. Many in situ manipulative experiments have reported that the vegetation response to climate change can be largely influenced by plant functional traits and soil nutrient availability. For example, in a climate simulation study of alpine grasslands, Henn et al. [19] found that alpine plants can adapt to climate change by shaping leaf traits. In a recent meta-analysis, soil nitrogen availability was found to be a determinant of terrestrial ecosystem productivity under changing climates [20]. However, the findings from local in situ experiments are always hard to be directly applied

to large-scale ecosystem management. Therefore, it is necessary to combine remote sensing technologies and field observations to gain insights into the mechanisms of how vegetation adapts to changing climate via plant and soil nutritional properties.

Plants can respond specifically and actively to environmental changes rather than only passively withstand external stresses [21]. According to the community functional ecology theories [22–24], plant seed germination, seedling growth, and individual development and survival, along with environmental gradients, are mainly regulated by functional traits at species and community levels [25–30]. Plant individuals can modify their water requirements by reducing leaf size, stomatal conductance, and photosynthetic rates in response to droughts [3,31,32]. At the community level, plants can alter the C:N:P stoichiometry among organs above- and belowground to offset physical inhibitions caused by warming or cooling [33,34], declined moisture [35–37], and changed nutrient availability [38]. For example, Jiang et al. [39] found that warming could substantially enhance N and P mineralization and consequently improve nutrient provision to plants in the Arctic tundra. Recently, Delgado-Baquerizo et al. [40] and Jiao et al. [41] also found that increased aridity, mainly due to warming, could reduce the concentrations of C and N but increase that of P in drylands. Fiedler et al. [42] also found that climate change could indirectly affect the trade-offs and synergies among different ecosystem functions by affecting soil nutrients and plant traits. These studies indicated that ecosystem responses to climate change are complicated and depend on abiotic and biotic factors [43]. Network analyses that include plant functional traits and physical environments together may improve our prediction of ecosystem functional changes across space and over time [44–46]. However, our understanding of the interactions of plant functional traits with soil nutrients of high-elevated drylands in response to climate variability is still limited.

In this study, we aimed to improve our understanding of how plant nutrient traits interact with low soil nutrient availability to regulate the sensitivity of desert scrubs in the Qaidam Basin, northeastern Qinghai-Tibetan Plateau, in response to climate variability. Specifically, we have (i) explored the patterns and trends of climate change and desert scrub coverage in the last decade, (ii) examined the differences in climatic sensitivity and its components for different desert scrub communities, and finally, (iii) investigated the networking paths of interactions between plant nutrient traits and soil nutrient availability to the components of desert scrubs' sensitivity to climate variability across the entire Qaidam Basin.

## 2. Materials and Methods

### 2.1. Study Area

The Qaidam Basin, with elevations ranging from 2640 m to 6000 m, is surrounded by the Kunlun, Qilian, and Altun Mountains and located in the northeastern Qinghai-Tibetan Plateau (90°16'E~99°16'E, 35°00'N~39°20'N, Figure 1). The area is characterized by an alpine arid continental climate, where the mean annual temperature (MAT) is generally below 5 °C and mean annual precipitation (MAP) is less than 200 mm [47]. The air relative humidity is between 30% and 40% throughout the year, while the average yearly sunshine duration can reach 3000 h in the Qaidam Basin. The annual average evaporation in the basin is between 1900 mm and 2600 mm [48]. Soil nutrients and moisture availability are low in desert scrublands in this area [49]. The vegetation has co-evolved with harsh physical conditions and is dominated by scrubs and semi-scrubs, such as *Kalidium foliatum*, *Salsola abrotanoides*, and *Ephedra sinica* [50]. Desert plants sprout in May and defoliate in early October; therefore, this period was usually defined as the plant growing season in recent studies [51].

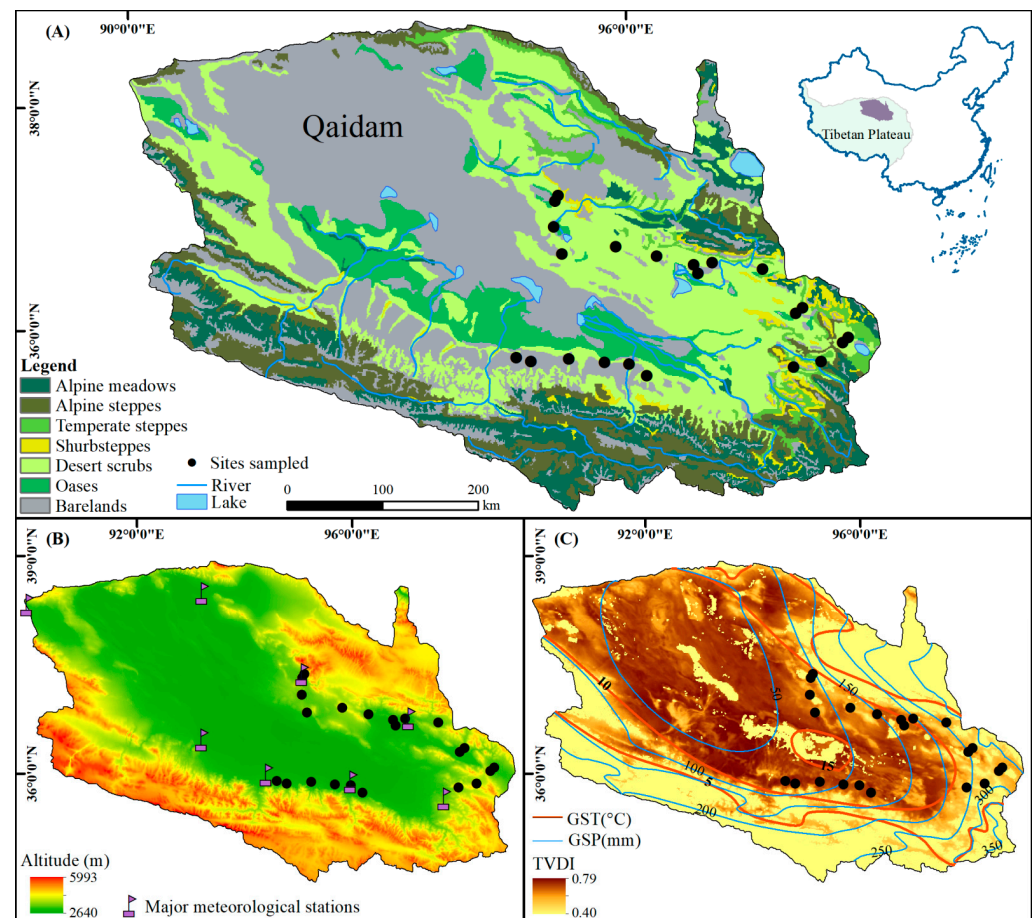


**Figure 1.** Vegetation (A), elevation and major meteorological stations (B), climate (C), and site locations (black dots) in the Qaidam Basin, Qinghai-Tibetan Plateau. In Panel C, GST and GSP refer to the average temperature and sum precipitation during the plant growing season, respectively, from May to October during 2000–2015. TVDI means the temperature vegetation dryness index.

## 2.2. Remote Sensing Data Collection and Processing

It is the key to choosing a suitable vegetation index for accurately examining and assessing vegetation dynamics under climate change. Recently, Zhang et al. [50] have evaluated the correlation between different vegetation indices and vegetation cover observed with UAV in the Qaidam Basin. They found that the Normalized Difference Vegetation Index (NDVI) performed much better than other indices such as ratio vegetation index (RVI), difference vegetation index (DVI), modified vegetation index (MVI), modified soil-adjusted vegetation index (MSAVI), and normalized difference greenness index (NDGI) in assessing vegetation cover. Therefore, in this study, the NDVI of the Moderate Resolution Imaging Spectroradiometer (MODIS) MOD13Q1 Products was used as a proxy for vegetation productivity of desert scrubs. We downloaded the NDVI data with a temporal resolution of 16 days and spatial one of 250 m for the Qaidam Basin for the period from 2000 to 2015 (<https://ladsweb.modaps.eosdis.nasa.gov/>, accessed on 1 October 2021). As NDVI is sensitive to soil background information, therefore, we used the Savitzky–Golay filter [52] to smooth the time-series NDVI and eliminate the contaminations caused by clouds, snow, and ice cover, following Li et al. [15]. The pixels whose peak NDVI value was less than 0.05 were classified as extremely sparse vegetation or barren lands. Those pixels were manually excluded from further analyses following the recent study of Yuan et al. [18] in Central Asia. Finally, the peak monthly NDVI generated by maximum value composites [53] was used to

describe the sensitivity and its components of desert scrub vegetation in the Qaidam Basin, Qinghai-Tibetan Plateau, to the variability of different climate variables.

### 2.3. Weather Data Collection and Processing

The monthly data of temperature and precipitation of the main meteorological stations within the Qaidam Basin (Figure 1B) yearly from May to September were downloaded and mapped for the period of 2000 to 2015. Seasonal and inter-annual fluctuations in temperature and precipitation, as well as their extreme values, were clearly shown in the supplementary Figure S1. It makes sense that the weather data from 2000–2015 are sufficient to reflect the climate fluctuations in the region. Therefore, we downloaded monthly temperature and precipitation of 200 meteorological stations located within and around the Qinghai-Tibetan Plateau from the China Meteorological Data Service Centre (<http://data.cma.cn/en>, accessed on 5 October 2021) for the plant growing seasons (yearly from May to October) between 2000 and 2015. First, the average temperature and sum precipitation during the plant growing seasons (termed as GST and GSP, respectively) were calculated for each station. In addition to monthly weather records, we interpolated GSP and GST into rasters with ANUSPLIN (The software is developed by Australian National University in Australia and the version is 4.3) [54] at a spatial resolution of 250 m to match the remote sensing data (see details below). A digital elevation model (DEM) with a 30 m resolution was used as the covariate, following Li et al. [55], who also confirmed that the interpolated climate rasters matched well the field observations across the northern Tibetan Plateau.

In this study, we used the temperature vegetation dryness index (TVDI) to explore the vegetation-drought relationship as recommended by Sandholt et al. [56] because it combines vegetation greenness (MODIS MOD13A2) and land surface temperature (MOD11A2). TVDI ranges from 0 to 1, with higher values indicating drier soils. We downloaded monthly TVDI data from the National Earth System Science Data Center (<http://www.geodata.cn>, accessed on 12 October 2021) and resampled it to match the spatial-temporal resolutions of climate and NDVI data. Finally, we used the Mann–Kendall tests [57,58] to examine the trends of GST, GSP, NDVI, and TVDI at the pixel scale between 2000 and 2015 (see more details in Figures S2–S5). The MK test outputs Z-values and slope, with positive and negative slope values representing increasing and decreasing trends.  $|Z| > 1.96$  reaches a significant level ( $\alpha = 0.05$ ).

### 2.4. Climatic Sensitivity Index of Desert-Scrubs

In this study, we used NDVI as an agent of desert-scrub coverage to explore its sensitivity to changes in GST, GSP, and TVDI. First, we transformed the time-series NDVI and climate variables into z-score anomalies using each variable's mean and standard deviation (Equation (1)).

$$Z = \frac{X - \bar{X}}{\sigma} \quad (1)$$

where Z is the standard score, X is the raw data,  $\bar{X}$  is the mean value of data, and  $\sigma$  is the standard deviation of data. Then, we used a principal component regression (PCR) to determine the relative importance of each climate variable in driving the monthly NDVI dynamic at the pixel scale. Principal components with significant relationships to climatic variables ( $p < 0.1$ ) were retained for the subsequent VSI calculations.

The climate weights ( $W_i$ ) were obtained by multiplying the loading scores of each variable with the corresponding PCR coefficients. Here, the weight of each climate variable was also rescaled to be between 0 and 1. Then we detrended each time-series variable and extracted its weight variance. The residuals of the mean-variance relationship between NDVI and climate variables were fitted using a linear-quadratic model, following Seddon et al. [14]. The residuals were normalized between 0 and 100. We take the  $\log_{10}$ -transformed ratios between NDVI variability and climate variables as the sensitivity metrics

( $S_i$ ). The NDVI logged for one month was used as the fourth variable to explore the time-lag effect of vegetation response to climate variability, following Seddon et al. [14].

$$VSI = \sum_{i=1}^3 W_i \times S_i \quad (2)$$

where VSI is the sum of the product of the weights of each climate variable ( $W_i$ ) and its sensitivity metrics ( $S_i$ ). We rescaled the VSI between 0 and 100 (unitless), and the larger the value, the more sensitive to climate variability. We constructed a 500 m buffer centered on each sample point. Thus, it makes sense that the specific VSI values of the pixels in the buffer area can serve as repeats for multiple comparisons among different scrub communities. Moreover, we calculated the VSI average of the pixels in the buffer area for each site and used it in multiple linear regressions and structural equation modeling across sites within the study area.

### 2.5. Plant Nutrient Traits and Soil Nutrient Availability

According to the 1:1,000,000 China Vegetation Atlas, which is available at the Resource and Environmental Science Data Center, Chinese Academy of Sciences (<http://www.resdc.cn/data.aspx?DATAID=122>, accessed on 1 May 2016), our field observations in 2016 at 22 sites covered seven main types of desert scrubs within the Qaidam Basin (Table 1). Plant nutrient traits and soil nutrient properties were measured to examine their potential regulating effects on the desert scrubs' sensitivity to climate variability.

We laid five 5 m × 5 m sample squares evenly along the diagonal in a relatively homogeneous area of 250 m × 250 m at each site, where the plant community was intact and undisturbed by human activities while the proportion of desert scrub plants was higher than 90% in the total vegetation cover. Healthy leaves were collected from at least five mature individuals for each scrub/semi-scrub species in each quadrat. Plant leaves were stored in a separate bag for each species during the field campaign and then dried at 70 °C for 48 h in the lab to a constant weight. Before chemical analyses, all dried leaves were grounded into fine powder through a 0.15 mm sieve and kept in brown glass bottles. Leaf total P (LTP, g kg<sup>-1</sup>) and K (LTK, g kg<sup>-1</sup>), respectively, were determined by Mo-Sb colorimetric method and flame spectrophotometer [59].

We randomly sampled three profiles of the 0–50 cm depth at each site, about a half kilogram for each sample. Soil samples were air-dried and sieved through a 100-mesh sieve to remove root fractions and gravel. Then, soils were grounded into fine powders and stored in brown glasses before chemical analyses [60]. Total soil and leaf nitrogen (STN and LTN, g kg<sup>-1</sup>) were determined by Kjeldahl method. Total soil and leaf phosphorus (STP and LTP, g kg<sup>-1</sup>) were measured with the Mo-Sb anti-spectrophotometry method, while total soil and leaf Kalium (STK and LTK, g kg<sup>-1</sup>) with the flame photometry method. Soil organic carbon (SOC, g kg<sup>-1</sup>) and leaf carbon (LC, g kg<sup>-1</sup>) were determined by the potassium dichromate oxidation–ferrous sulfate titrimetric method.

**Table 1.** Locations, the most dominant species and their relative coverage (DSC), climate conditions, soil properties, and plant nutrient traits at each site sampled in 2016 across the Qaidam Basin. GST and GSP refer to the average temperature and precipitation during the plant growing season. Soil properties included the contents of organic carbon (SOC), total nitrogen (STN), total phosphorus (STP), and total potassium (STK) of topsoils at the 0–50 cm depth. Plant nutrient traits were the community weighted means (CWMs) of leaf carbon (LC), total nitrogen (LTN), total phosphorus (LTP), and total potassium (LTK) in the leaves of all plants at each sampling site.

Site	Long (°E)	Lat. (°N)	Alt. (m)	Dominant Species	DSC (%)	GST (°C)	GSP (mm)	SOC (g kg <sup>-1</sup> )	STN (g kg <sup>-1</sup> )	STK (g kg <sup>-1</sup> )	STP (g kg <sup>-1</sup> )	LC (g kg <sup>-1</sup> )	LTN (g kg <sup>-1</sup> )	LTP (g kg <sup>-1</sup> )	LTK (g kg <sup>-1</sup> )
Site1	95.091	36.346	2890	<i>Sympegma regelii</i>	53.0	16.4	66	1.48	0.09	14.00	0.45	326.60	20.95	1.00	14.72
Site2	95.267	36.325	2970	<i>Ephedra sinica</i>	65.0	15.8	72	1.21	0.11	14.67	0.43	311.36	16.67	0.45	8.16
Site3	95.703	36.381	2850	<i>Ephedra sinica</i>	48.0	16.8	73	1.76	0.09	15.27	0.46	397.40	15.09	0.65	11.13
Site4	96.126	36.378	2765	<i>Tamarix chinensis</i>	100.0	17.3	79	3.91	0.14	20.46	0.35	348.00	19.25	0.92	7.88
Site5	96.413	36.382	2855	<i>Krascheninnikovia ceratoides</i>	50.0	16.7	92	2.20	0.12	17.29	0.49	307.20	21.28	2.10	18.18
Site6	96.630	36.293	2850	<i>Haloxylon ammodendron</i>	100.0	16.4	101	3.52	0.07	16.27	0.43	132.00	30.45	1.36	28.97
Site7	98.329	36.469	3320	<i>Kalidium foliatum</i>	80.0	12.2	224	3.23	0.44	19.09	0.49	576.00	23.10	1.28	15.68
Site8	98.648	36.536	3530	<i>Kalidium foliatum</i>	59.0	10.4	264	6.16	0.51	18.74	0.46	353.51	22.87	1.63	17.19
Site9	98.883	36.723	3175	<i>Kalidium foliatum</i>	100.0	12.3	261	7.26	1.13	19.84	0.54	375.00	22.20	1.72	16.88
Site10	98.947	36.773	3070	<i>Kalidium foliatum</i>	65.0	13.1	257	4.25	0.43	18.14	0.53	451.50	33.84	1.88	9.71
Site11	98.312	36.962	2945	<i>Sympegma regelii</i>	27.0	14.5	214	4.58	0.40	17.65	0.52	338.68	20.31	1.94	23.31
Site12	98.390	37.017	3130	<i>Kalidium foliatum</i>	61.0	13.0	236	4.58	0.40	17.92	0.49	492.66	21.99	0.80	14.55
Site13	97.886	37.344	3205	<i>Salsola abrotanoides</i>	56.0	12.8	222	6.38	0.58	15.77	0.48	233.33	30.24	1.37	16.91
Site14	97.284	37.366	2970	<i>Sympegma regelii</i>	70.0	14.6	172	5.35	0.38	17.12	0.37	307.80	28.65	2.33	13.93
Site15	97.127	37.258	2860	<i>Krascheninnikovia ceratoides</i>	56.0	16.3	146	2.20	0.29	18.29	0.42	440.00	23.90	1.86	16.50
Site16	97.068	37.333	2905	<i>Kalidium foliatum</i>	83.33	15.8	149	4.90	0.46	19.04	0.44	384.00	26.95	1.83	13.69
Site17	96.623	37.384	2980	<i>Sympegma regelii</i>	60.00	15.7	126	3.30	0.34	19.08	0.47	403.80	23.42	1.36	23.54
Site18	96.135	37.440	3620	<i>Salsola abrotanoides</i>	66.67	11.2	135	6.71	0.58	20.40	0.66	346.67	23.57	1.02	20.15
Site19	95.395	37.855	3310	<i>Sympegma regelii</i>	40.00	13.1	91	7.33	0.39	22.71	0.58	321.60	14.70	2.90	21.44
Site20	95.364	37.800	3190	<i>Krascheninnikovia ceratoides</i>	100.00	13.8	85	12.38	0.29	23.09	0.49	528.00	25.67	1.37	34.63
Site21	95.381	37.565	3185	<i>Krascheninnikovia ceratoides</i>	50.00	14.1	82	3.25	0.13	18.56	0.50	330.00	20.65	3.40	17.60
Site22	95.506	37.328	3035	<i>Ephedra sinica</i>	40.00	15.3	76	2.31	0.12	15.52	0.56	444.60	16.19	2.17	10.66

## 2.6. Plant Functional Trait Diversity

Our plant nutrient traits referred to the contents of N, P, K, and C in leaves (LTN, LTP, LTK, and LC) for all species sampled (Table 1). We calculated community-weighted means (CWMs) to describe the regulating effects of plant nutrient trait diversity on desert scrubs' sensitivity to climate variability (see Equations (2) and (3)). CWMs are essential for understanding community reorganization in response to environmental filtering [61] and are widely recommended and used in plant functional ecology research [62].

$$CWM_j = \sum_{i=1}^n P_{ij}T_{ij} \quad (3)$$

where  $P_{ij}$  is the relative cover of species  $i$  in sample site  $j$ ;  $T_{ij}$  is the mean of trait values of species  $i$  in sample site  $j$ ;  $CWM_j$  is the community-weighted mean of traits of each species in sample site  $j$ .

## 2.7. Statistical Analyses

First, with the Mann–Kendall test [57,58], we examined the trends of GST, GSP, TVDI, and NDVI between 2000 and 2015 at the pixel scale. Moreover, we extracted the yearly value and trends of GST, GSP, TVDI, and NDVI based on each site's geographical coordinate records at the pixels where we performed field surveys. Thus, we compared the medians of climate and vegetation variables and their trends among the seven types of desert scrubs (see more details in Figures S2–S5).

Second, we calculated the VSI of 2000–2015 based on principal component regressions and used a red–green–blue (RGB) composition map to show the relative contribution of GST, GSP, and TVDI to the climatic sensitivity of desert scrubs at the pixel scale. We also extracted the VSI and its components to each site and examined the difference in them at the community level with the Wilcoxon test [63].

Next, we divided the data into three groups: VSI as the response variable and leaf traits (LTN, LTP, LTK, LC) and soil attributes (STN, STP, STK, SOC) as potential explanatory variables. We examined the normality of the data containing response and predictor variables and normalized these data in R using a scale function (see Equation (1)). Moreover, we examined the correlation between the responders and predictors using the corrplot package (version 0.92) [64] in R. The multivariate linear model was applied to investigate the main effects of leaf and soil nutrient attributes on the variation of VSI. In this step, we also determined the multicollinearity of each factor based on the variance inflation factor (VIF) [65]. Thus, the relative importance of each explanatory can be disentangled as the fraction of the variance VSI explained in the best-fitted model.

Finally, structural equation modeling (SEM) [66] was used to explore how vegetation traits and soil nutrients drive changes in VSI using the lavaan package (version 0.6.1) [67]. Stepwise backward selections were used to remove the least significant term until the best-fitted model was picked out. All statistical analyses were performed in R (The software is developed by R Core Team in Austria and the version is 4.1.1) [68], and maps were generated with ArcGIS (The software is developed by the Environment System Research Institute in America and the version is 10.2) [69].

## 3. Results

### 3.1. Vegetation Sensitivity Index and Its Contributors

The overall VSI of desert scrubs is low (15.0) and distributed unevenly across the Qaidam Basin. The VSI was greater than 30 at only 1.18% pixels scattered near the foothills and riverbanks (Figures 1A and 2A, Table 2). The relative contribution of each climatic variable also varies heterogeneously across space. Specifically, in the western and northeastern areas, vegetation is more sensitive to changes in GSP. However, the desert scrubs in the southern and northern areas were mainly affected by temperature dynamics. In the eastern part, desert scrubs were jointly controlled by GSP and TVDI (Figure 2B). Moreover, the desert scrubs in the central region were driven by GST and TVDI together.

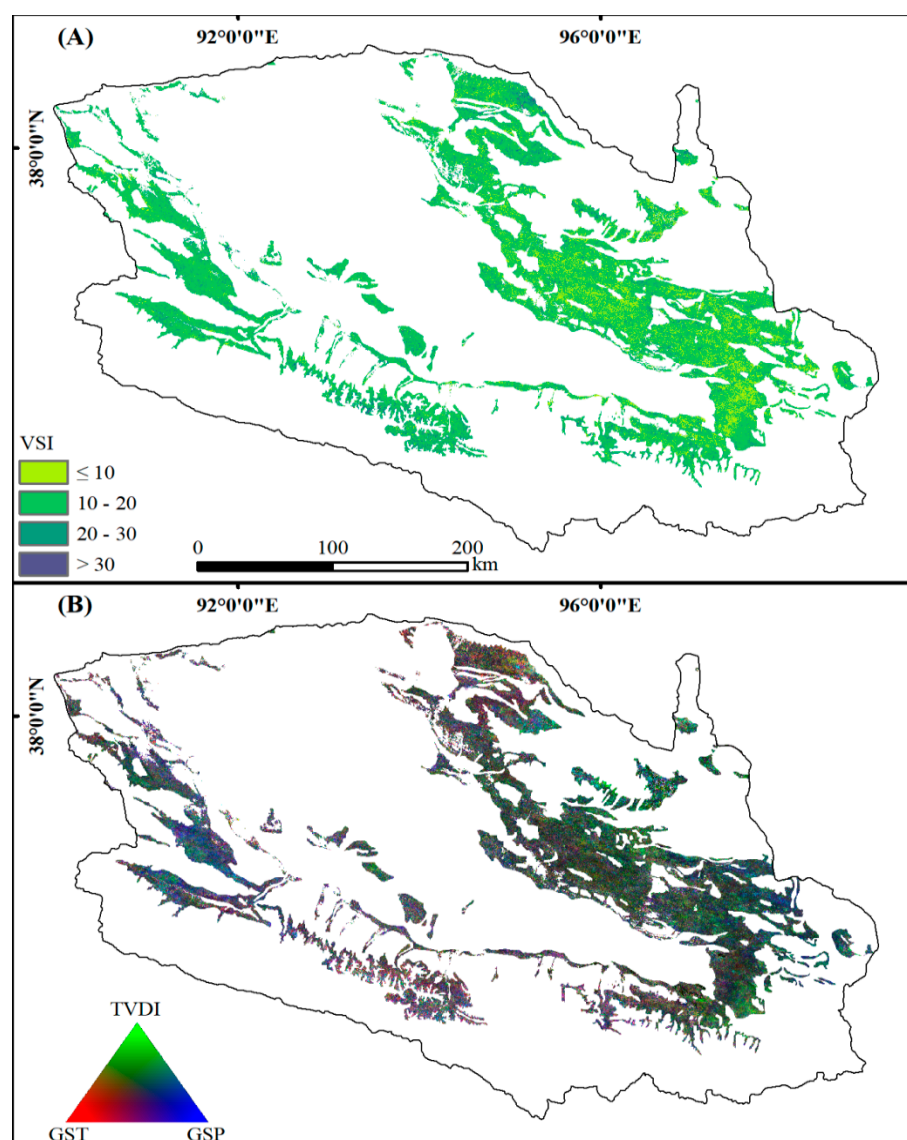


**Figure 2.** Vegetation Sensitivity Index (VSI, (A)) and its contributions (B) from the temperature and precipitation during the plant growing season (GST and GSP, respectively, in red and blue) and temperature vegetation dryness index (TVDI, in green).

**Table 2.** Vegetation Sensitivity Index (VSI) among different desert scrub communities across the Qaidam Basin.

	<i>Haloxylon ammodendron</i> (%)	<i>Tamarix chinensis</i> (%)	<i>Krascheninnikovia ceratoides</i> (%)	<i>Sympegma regelii</i> (%)	<i>Ephedra sinica</i> (%)	<i>Salsola abrotanoides</i> (%)	<i>Kalidium foliatum</i> (%)	Others (%)	Total (%)
VSI ≤ 10	3.24	1.10	4.57	0.32	0.69	4.07	0.83	2.45	17.32
10 < VSI ≤ 20	8.00	6.96	16.64	1.39	2.88	20.70	5.46	7.88	70.27
20 < VSI ≤ 30	0.96	1.28	2.78	0.16	0.41	3.64	0.80	1.09	11.23
VSI > 30	0.09	0.10	0.36	0.01	0.04	0.40	0.06	0.11	1.18

Communities dominated by *Haloxylon ammodendron* and *Tamarix chinensis* were more sensitive to climate variability than others (Figure 3A). The climatic weights vary among desert-scrub types. Communities dominated by *Tamarix chinensis* were more sensitive to GST than others (Figure 3B), while communities dominated by *Haloxylon ammodendron* were more vulnerable to GSP (Figure 3C). In response to changes in TVDI, communities dominated by *Tamarix chinensis* were slightly more vulnerable than those dominated by

*Haloxylon ammodendron*. However, both communities were more sensitive than other desert scrub communities across the Qaidam Basin (Figure 3D).

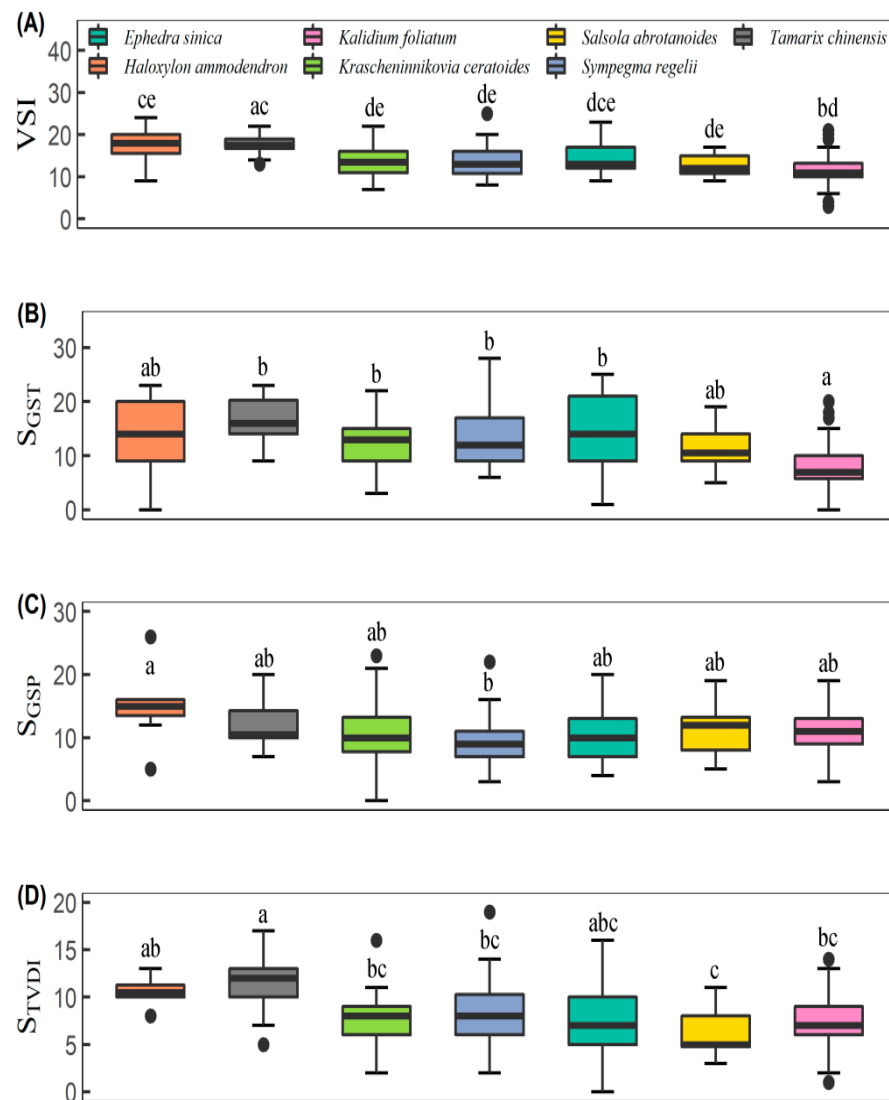


**Figure 3.** Comparisons of VSI (A) and its climatic weights among desert scrub communities. Panels (B–D) displayed the weights of mean temperature and sum precipitation during the plant growing season (noted as  $S_{GST}$  and  $S_{GSP}$ , respectively) as well as the temperature vegetation dryness index ( $S_{TVDI}$ ). Different lowercase letters indicate significant differences among species.

### 3.2. Effects of Soil and Plant Properties on VSI

We found that VSI strongly correlated with the weights of GST ( $S_{GST}$ ,  $r = 0.81$ ) and droughts ( $S_{TVDI}$ ,  $r = 0.65$ , Figure S6).  $S_{GST}$  was negatively correlated with STN ( $r = -0.53$ ) and LTN ( $r = -0.51$ ). The weight of GSP ( $S_{GSP}$ ) was negatively correlated with LC ( $r = -0.49$ ). Moreover, SOC had strong correlations with  $S_{GST}$  ( $r = -0.53$ ), STK ( $r = 0.74$ ), LTK ( $r = 0.59$ ), and STN ( $r = -0.48$ ), respectively. Across different dominant species of the 22 sites surveyed in this study, we only found that  $S_{GST}$  declined linearly with increasing STN and LTN (Figures 4 and 5) while  $S_{GSP}$  declined linearly with increasing STP and LC (Figures 4 and 5).

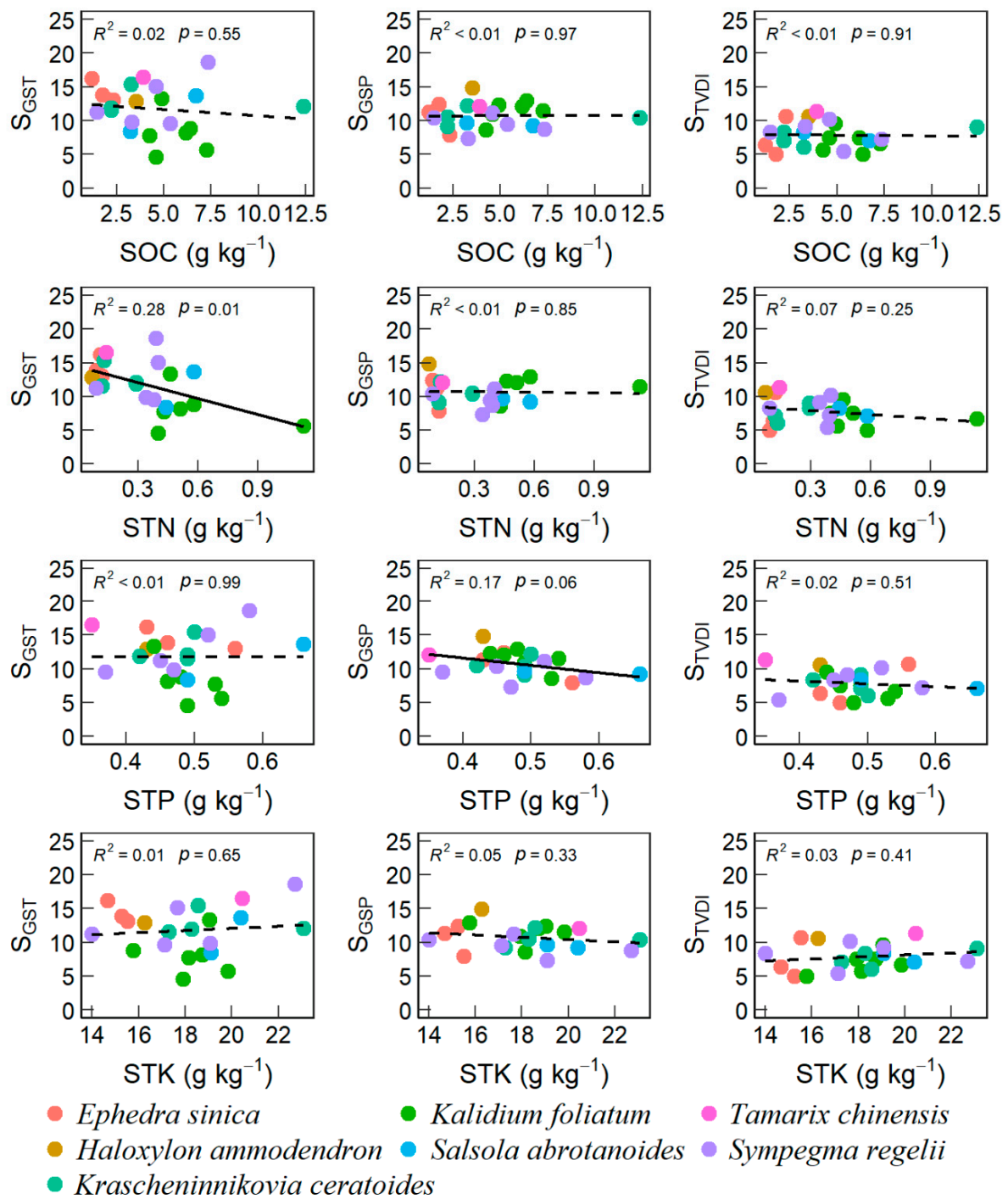
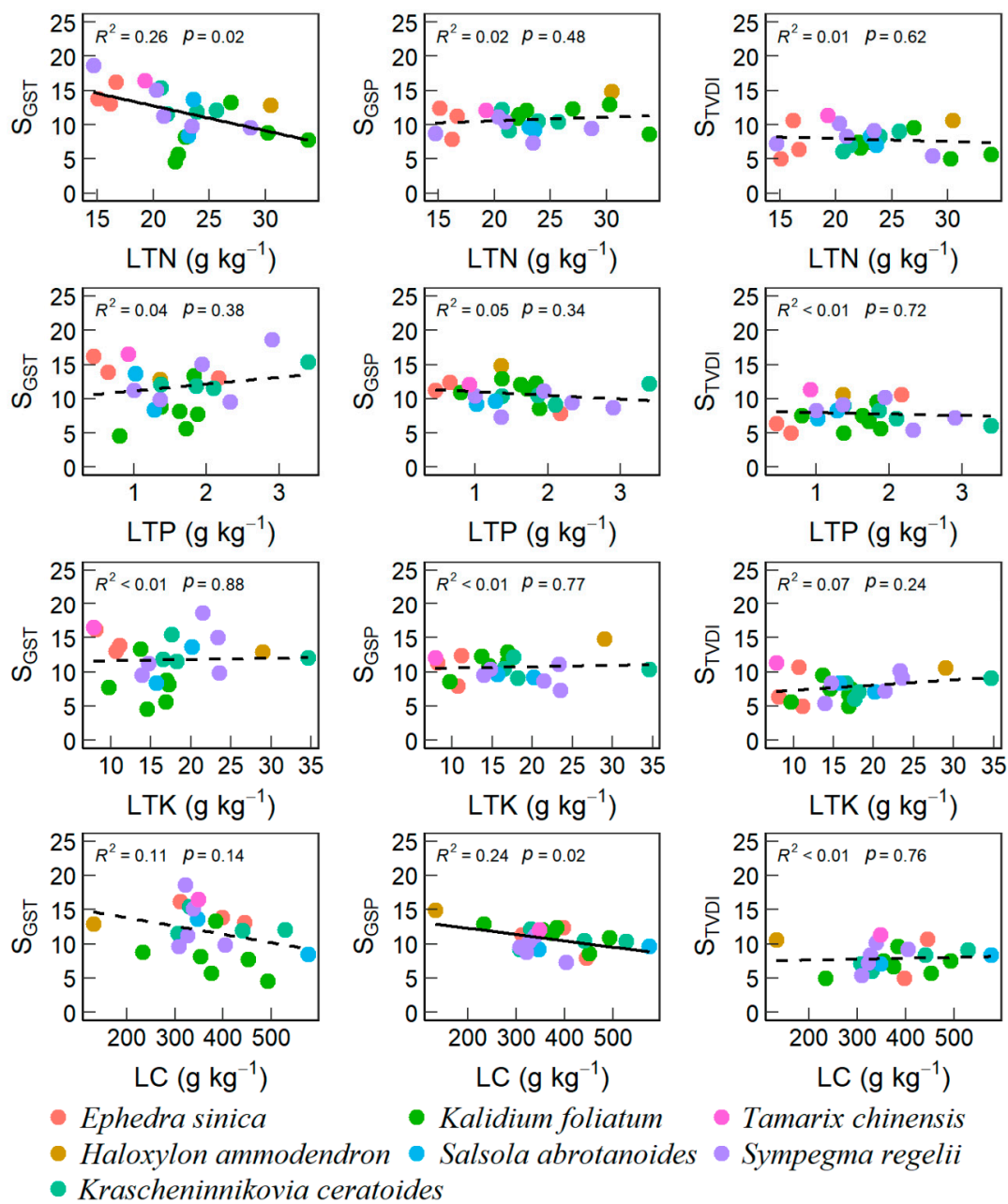


Figure 4. Trends of vegetation sensitivity index and its contributions with soil nutrients.



**Figure 5.** Trends of vegetation sensitivity index and its contributions with leaf nutrients.

However, we also found differential responses, linear, U-shaped, and unimodal, for different top-dominant species along the soil and foliar nutrient gradients (Figures S7 and S8). When examining the relationships of sensitivity components with soil nutrients, we only found that the  $S_{GST}$  of *Kalidium foliatum* and  $S_{TVDI}$  of *Sympegma regelii* had unimodal relationships with SOC and STP, respectively, at a marginal significance level ( $p < 0.1$ , Figure S7). When examining the relationships of sensitivity components with foliar nutritional traits, we found a significant unimodal relationship between  $S_{TVDI}$  and LC for *Sympegma Regelii* ( $p < 0.05$ , Figure S8), a marginally positive linear relationship between  $S_{GSP}$  and LTK for *Kalidium foliatum* ( $p < 0.1$ , Figure S8), a significant unimodal relationship between  $S_{GSP}$  and LTN for *Kalidium foliatum*, and a marginally positive linear relationship between  $S_{GST}$  and LTP for *Krascheninnikovia ceratoides* ( $p < 0.1$ , Figure S8).

STN and LC explained 42.9% of the variance in VSI across different desert scrubs ( $p < 0.05$ , Table 3).  $S_{GST}$  was significantly affected by STN and LC, which accounted for 49.0% of the variance in  $S_{GST}$  ( $p < 0.01$ , Table 3). In addition to STN and LC, LTN and STK

affected  $S_{GST}$  marginally, respectively, to explain 9.11% and 7.62% of the variance in  $S_{GST}$  ( $p = 0.053$  and  $0.073$ , respectively, Table 3).  $S_{GSP}$  was affected by LC and STP marginally, with 14.0% and 18.9% of its variance explained by LC and STP ( $p < 0.1$ , Table 3). Neither soil nutrients nor plant leaf traits influenced  $S_{TVDI}$  in this study ( $p > 0.05$ , Table 3).

**Table 3.** Main effects of soil nutrient availability and plant nutrient traits on vegetation sensitivity index (VSI) of desert scrubs across the Qaidam Basin. Abbreviations were the same as in Table 1. d.f., the degree of freedom; F, variance ratio;  $p$ , significance level;  $\eta^2$ , Eta squared, the percentage of sum squares explained. The difference significant at the 0.01 and 0.05 levels were labeled with \*\* and \*, respectively.

Predictor d.f.	VSI, $R^2 = 0.57$			$S_{GST}$ , $R^2 = 0.74$			$S_{GSP}$ , $R^2 = 0.45$			$S_{TVDI}$ , $R^2 = 0.21$		
	F	$p$	$\eta^2$ (%)	F	$p$	$\eta^2$ (%)	F	$p$	$\eta^2$ (%)	F	$p$	$\eta^2$ (%)
SOC 1	0.29	0.597	0.98	0.89	0.362	1.80	0.00	0.970	0.01	0.01	0.910	0.07
STN 1	7.74	0.016 *	25.88	14.87	0.002 **	29.90	0.07	0.795	0.30	1.54	0.236	8.34
STP 1	0.14	0.710	0.48	2.01	0.180	4.04	4.43	0.055	18.88	0.09	0.764	0.51
STK 1	1.31	0.273	4.39	3.79	0.073	7.62	1.94	0.188	8.25	1.82	0.200	9.83
LTN 1	1.35	0.266	4.53	4.53	0.053	9.11	0.04	0.850	0.16	0.00	0.963	0.01
LTP 1	0.00	0.946	0.02	1.11	0.311	2.23	0.08	0.788	0.32	0.45	0.516	2.41
LTK 1	0.96	0.345	3.22	0.05	0.831	0.10	0.63	0.443	2.67	1.57	0.232	8.50
LC 1	5.09	0.042 *	17.02	9.48	0.009 **	19.06	3.27	0.094	13.96	0.02	0.903	0.08

### 3.3. Causal Network of Plant Traits and Soil Nutrients to VSI under Climate Variability

Structural equation modeling revealed the causal networking paths among plant and soil nutrient traits and climate weights to the sensitivity of desert scrubs across the Qaidam Basin (Figure 6). STN, LC, and LTN had direct adverse effects on  $S_{GST}$ . In contrast, STK had a significant positive effect on  $S_{GST}$ . LC had direct adverse effects on  $S_{GSP}$ , accounting for about 24% of its total variance. STN had direct adverse effects on  $S_{TVDI}$ , while STK had a significant positive effect on  $S_{TVDI}$ . However, STN and STK accounted for only 16% of the variance in  $S_{TVDI}$ .

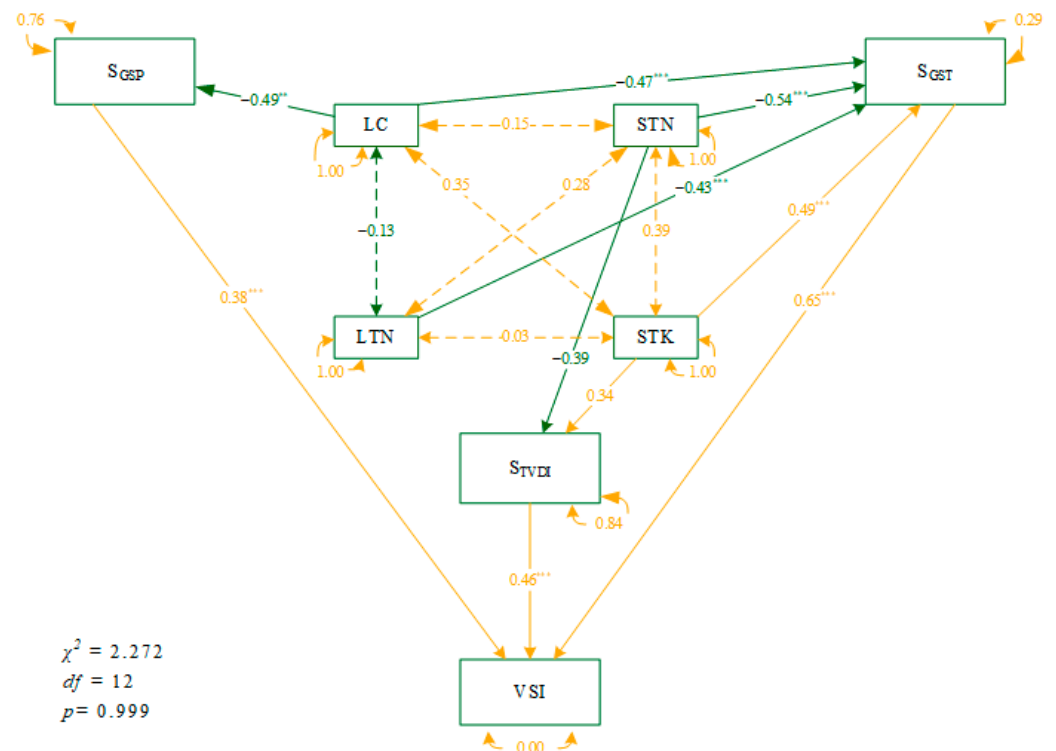


**Figure 6.** Structural equation modeling reveals the direct and indirect effects of leaf traits and soil properties on VSI and its components of desert scrubs across the Qaidam Basin. Notes are the same as

in Table 1. The orange and dark-green lines represent the positive and negative influences, respectively. The difference significant at the 0.001 and 0.01 levels were indicated with \*\*\* and \*\*, respectively.

## 4. Discussion

### 4.1. Climate Sensitivity among Different Desert Scrubs

In this study, we mapped the climate sensitivity of desert scrubs in the Qaidam Basin using principal component regressions (Figure 2). We found that the climatic sensitivity of desert scrubs in this study was not high as expected. However, this finding is consistent with Seddon et al. [14] and Yuan et al. [18], and they found that arid deserts across the globe and Central Asia, respectively, were not as sensitive to climate dynamics. This phenomenon may have resulted from the strong memory effect of desert plants (Figure S9). The vegetation memory effect generally refers to the fact that previous environmental conditions can strongly influence the current ecosystem [70]. Ogle et al. [71] quantified ecological memory in vegetation and ecosystem processes in arid and semi-arid regions and found when the vegetation's memory effects were considered, 18–28% more of the variance in a given responsible variable could be explained. Seddon et al. [14] also found such a strong memory effect in global drylands' sensitivity to climate change. Moreover, the low climatic sensitivity of desert scrubs in the Qaidam Basin was also likely due to the relatively slow warming during the last decade (Figure S2), a rate of only 0.06 °C per decade. This finding was also confirmed by Easterling and Wehner [72] that at the beginning of the 21st century, there would be a 10- to 20-year warming hiatus. Overall, the stable climatic conditions may be another explanation for the low climate sensitivity of desert scrubs in the Qaidam Basin.

Although the desert scrubs were not sensitive as expected to climate change, we also found high species-dependency for the seven community types involved in this study. Specifically, we found that scrub communities with tall plant individuals, such as *Tamarix chinensis* communities and *Haloxylon ammodendron* communities, were more sensitive to climate change (Figure 3). Similarly, Zhu et al. [73] have found that northern China's trees and tall shrubs are more vulnerable to climate change. This is because taller plants have predictably wider water-conducting conduits, so they are more vulnerable to conduction-blocking embolisms [74]. Therefore, the response of different plant communities to climate change is influenced by the functional traits evolved to adapt to long-term environmental changes. However, vegetation also reacts and adjusts positively to environmental stresses [21]. Environmental-vegetation interactions have shaped scrub communities with different tolerance, and the response of these scrub communities to climate variability varies widely in the Qaidam Basin. The environmental filtering hypothesis predicts that, excluding biotic interactions, only the species that have already evolved with specific functional or phenotypic traits for survival, such as tolerance or avoidance of dryland plants to extreme water deficits [21,75]. This might be the reason for the differences in the relative weight of temperature ( $S_{GST}$ ), precipitation ( $S_{GSP}$ ), and drought ( $S_{TVDI}$ ) found among the top-dominant species (Figure 3).

### 4.2. Desert-Scrubs' VSI Correlated with Soil and Leaf Nutrients

Warming is one of the important drivers for community structural and functional changes in drylands. Here, we found that STN, STK, LTN, and LC were closely related to the  $S_{GST}$  of vegetation (Table 3) and together explained more than 65% of the variance in  $S_{GST}$  (Table 3). This might be because warming can enhance soil microorganism activities, promote SOM decomposition and N mineralization, and thereby increase the supply and availability of soil nutrients [76–78]. In addition to STN and STK, warming can also enhance the activity and supply of K ions in soil solution [79].

In addition to soil nutrients, we also found that  $S_{GST}$  generally declined with increasing LTN and LC (Figure 5), indicating a high photosynthetic rate with high LTN and LC can

mitigate the negative effects of warming. LTN and LC are usually used to describe the photosynthetic activity under manipulated stresses in experimental studies [80,81]. Our findings were partly consistent with Li et al. [15] that high-elevated grasslands have greater  $S_{GSP}$  than those in low-elevations on the Tibetan Plateau. Dryland plants can increase leaf photosynthetic enzymes by enhancing LTN to promote photosynthetic rate and water use efficiency [82–84]. Moreover, our findings confirmed that the relationships of sensitivity climatic components with soil and foliar nutrients varied among different top-dominant species (Figures S7 and S8), likely due to species niche overlapping and differentiation.

Water availability is the main limiting factor for desert vegetation, and we found that STP and LC were the main factors affecting vegetation  $S_{GSP}$ , explaining 18.8% and 13.96% of the variation in  $S_{GSP}$ , respectively. P is an important element that affects vegetation growth, development, and metabolism; however, it can be readily combined with  $Ca^{2+}$  in arid soils and then is hard to be uptaken by plants. Pulsed precipitation in drylands can influence P transport, transformation, and availability through biochemical processes that control organophosphorus mineralization [85,86]. This might be the reason for the declining  $S_{GSP}$  with increasing STP (Figure 4) in our study.

LC is closely related to the photosynthesis of vegetation. Under drought conditions, vegetation reduces its water loss by decreasing leaf area and lowering light saturation point, which results in impaired ATP synthesis and reduced carboxylase activity, resulting in impaired leaf photosynthesis and thus reduced LC fixation [87]. Pulsed precipitation can briefly mitigate vegetation drought conditions and provide good moisture conditions for vegetation photosynthesis, thus increasing LC accumulation. This is why we also found that  $S_{GSP}$  declined with increasing LC content across different species (Figure S8). In addition, we also found that the LC of the seven arid scrub species was concentrated in the 300–400 g kg<sup>-1</sup> interval, which may imply the coexistence of species has evolved with overlapped niches to successfully survive in the Qaidam Basin, Qinghai-Tibetan Plateau.

It is worthy to note that neither soil nor plant nutritional properties alone can well explain the variance in  $S_{TVDI}$ , which describes the availability of soil moisture, in other words, the combining effects of temperature and precipitation. In this study, we found that  $S_{TVDI}$  could be associated with STN and STK at the same time (Figure 6). Both STN and STK could explain 16% of the variance in  $S_{TVDI}$  across different species and sites. Soil water deficit caused by decoupling temperature and precipitation can limit soil microbial activity and slow down soil N mineralization [88]. Moreover, a drying environment with high temperatures and limited precipitation can also exacerbate the volatilization of gaseous N and lead to high evaporative demand [89], which in turn reduces the availability of STN [90]. Dry conditions can enhance soil inorganic N content [91]; however, they are hardly taken up by plants due to diffusion limitations [92]. The uptake of potassium by vegetation is dependent on soil moisture [93]; soil water deficit reduces soil potassium release capacity and availability [94] and inhibits soil potassium mobility, limiting potassium uptake by vegetation.

#### 4.3. The Networks of Direct and Indirect Environmental Influences on VSI

The response of vegetation to climate change is characterized by the integrated effect of multiple factors and processes, forming complex and specific climate-species relationships [95,96]. In this study, we found that soil and foliar nutrient properties affect the scrub communities' climate sensitivity by regulating different climate sensitivity components. Even more, such regulating effects are dependent on the spatial scale, across sites, or for a given species. Finally, we found that the effect of soil nutrient effectiveness on VSI was greater compared to leaf nutrient effectiveness. The path strength of STK and STN on  $S_{GSP}$  were greater than that of LC and LTN (Figure 6), and the explanatory power of STK and STN on the variance in  $S_{GSP}$  (37.52%) was greater than that of LC and LTN (28.17%, Table 3). Soil nutrients provide indispensable nutrients for the growth and development of vegetation, and the decoupling of soil nutrient cycles due to climate warming may negatively affect dryland ecosystem services [40]. We should pay attention to the role of

soil nutrients in drylands to maintain ecosystem stability. Therefore, in the future, the dependent and combining effects of biotic and abiotic factors on vegetation's sensitivity and vulnerability should be well examined and disentangled.

#### 4.4. Limitations and Future Work

In this study, we integrated remote sensing data and field measurements together to investigate the mechanisms behind desert scrub's sensitivity to climate change in the Qaidam Basin, Qinghai-Plateau. However, there are still several uncertainties in this study. First, there might be a scaling-mismatch problem between remote sensing data and field measurements. Indeed, NDVI can be used to reflect the information on all vegetation in the whole region. Limited by budgets, only dominant desert scrub plants were sampled and measured for functional traits. Herbaceous plants were not fully considered in field observations. This may affect the accuracy of CWMs of plant functional traits and lead to some bias in the interpretation of community climate sensitivity. In further studies, both scrubs and herbaceous plants should be well considered because they have differential strategies to adapt to changes in physical circumstances.

In addition, this study only considered several soil nutrients and failed to take into account the effects of microorganisms and trace elements in soils. A recent review suggests that soil microbes dominate soil life activities by mediating nutrient cycling, decomposing organic matter, inhibiting plant diseases, influencing soil structure, and maintaining vegetation productivity, are major drivers of soil ecosystem change, and have game-changing potential in restoring soil function [97]. Moreover, soil trace elements are directly involved in the metabolic activities of organisms and influence the growth and development of vegetation, and have received increasing attention globally [98]. Therefore, future studies should also integrate the effects of multiple factors to obtain a more comprehensive understanding of the vegetation–climate relationship.

## 5. Conclusions

This study assessed and disentangled the sensitivity and its components of desert scrubs to climate variability with the time series of NDVI and weather data at the large scale crossing the Qaidam Basin. The regulatory mechanisms of plant and soil functional/nutritional traits behind the desert scrub's climate sensitivity were investigated and compared among multiple communities dominated by different plant species. The results confirmed that the sensitivity of vegetation to temperature change was mainly regulated by the contents of leaf carbon and nitrogen as well as soil nitrogen and potassium. In contrast, the sensitivity of vegetation to precipitation change was regulated by the contents of leaf carbon and soil total nitrogen. Neither soil nutrients nor plant foliar traits alone can well explain scrubs' sensitivity to droughts. Plant foliar traits and soil nutrient properties indirectly regulate the different components of vegetation's climate sensitivity. Due to harsh physical circumstances in the Qaidam Basin and limited available funds, a scaling-mismatch problem might still exist between remote-sensing data and field measurements in this study. Anyway, this study combined soil and plant functional traits together to provide a new perspective to investigate the mechanisms behind desert vegetation dynamics under climate change when assessed with large-scale remote-sensing data. These findings also highlighted the necessity to make management and conservation strategies specifically according to the different factors that regulate the vegetation–climate relationship among different plant communities.

**Supplementary Materials:** The following supporting information can be downloaded at: <https://www.mdpi.com/article/10.3390/rs14184601/s1>.

**Author Contributions:** J.W. and H.C. conceived ideas and designed field protocols. B.C., J.W. and M.L. collected data. B.C. and H.C. performed chemical analyses. J.W. and B.C. analyzed data, prepared figures, and led the writing. M.L., S.F., M.C.M., A.N., K.W., B.T. and H.C. interpreted the results. All authors have read and agreed to the published version of the manuscript.

**Funding:** This research was jointly supported by the Second Tibetan Plateau Scientific Expedition and Research (STEP, 2019QZKK1002), the Innovation Talent Exchange of Foreign Expert Program under the Belt and Road Initiative (DL2021056001L), the Key Project of the Hebei Normal University (L2021Z05) and the National Natural Sciences Foundation of China (41877448 and 40971118).

**Acknowledgments:** J.W. had been funded with a two-year scholarship from January 2017 to April 2019 by the Alexander von Humboldt Foundation in Germany. J.W. has been supported by the Young Talent Scientist Program of the Chinese Academy of Agricultural Sciences since December 2019. S.F. was funded by the Deutsche Forschungsgemeinschaft (DFG, project number 192626868–SFB 990/2-3). We appreciated the valuable comments and suggestions given by Ben Niu and Zhipeng Wang, and Yun Jäschke on the first draft of this manuscript.

**Conflicts of Interest:** The authors declare that they have no known competing financial interests or personal relationships that could have influenced the work reported in this paper.

## References

1. Reynolds, J.F.; Smith, D.M.; Lambin, E.F.; Turner, B.L., 2nd; Mortimore, M.; Batterbury, S.P.; Downing, T.E.; Dowlatabadi, H.; Fernandez, R.J.; Herrick, J.E.; et al. Global desertification: Building a science for dryland development. *Science* **2007**, *316*, 847–851. [[CrossRef](#)] [[PubMed](#)]
2. Millennium Ecosystem Assessment. *Ecosystems and Human Well-Being: Wetlands and Water*; Island Press: Washington, DC, USA, 2005; Volume 5.
3. Berdugo, M.; Delgado-Baquerizo, M.; Soliveres, S.; Hernandez-Clemente, R.; Zhao, Y.; Gaitan, J.J.; Gross, N.; Saiz, H.; Maire, V.; Lehmann, A.; et al. Global ecosystem thresholds driven by aridity. *Science* **2020**, *367*, 787–790. [[CrossRef](#)] [[PubMed](#)]
4. Huang, J.; Li, Y.; Fu, C.; Chen, F.; Fu, Q.; Dai, A.; Shinoda, M.; Ma, Z.; Guo, W.; Li, Z.; et al. Dryland climate change: Recent progress and challenges. *Rev. Geophys.* **2017**, *55*, 719–778. [[CrossRef](#)]
5. Vicente-Serrano, S.M.; Zouber, A.; Lasanta, T.; Pueyo, Y. Dryness is accelerating degradation of vulnerable shrublands in semiarid Mediterranean environments. *Ecol. Monogr.* **2012**, *82*, 407–428. [[CrossRef](#)]
6. Huang, J.P.; Yu, H.P.; Guan, X.D.; Wang, G.Y.; Guo, R.X. Accelerated dryland expansion under climate change. *Nat. Clim. Chang.* **2016**, *6*, 166–171. [[CrossRef](#)]
7. Barbier, E.B.; Hochard, J.P. Land degradation and poverty. *Nat. Sustain.* **2018**, *1*, 623–631. [[CrossRef](#)]
8. Tietjen, B.; Schlaepfer, D.R.; Bradford, J.B.; Lauenroth, W.K.; Hall, S.A.; Duniway, M.C.; Hochstrasser, T.; Jia, G.; Munson, S.M.; Pyke, D.A.; et al. Climate change-induced vegetation shifts lead to more ecological droughts despite projected rainfall increases in many global temperate drylands. *Glob. Chang. Biol.* **2017**, *23*, 2743–2754. [[CrossRef](#)]
9. Hantson, S.; Huxman, T.E.; Kimball, S.; Randerson, J.T.; Goulden, M.L. Warming as a driver of vegetation loss in the Sonoran desert of California. *J. Geophys. Res.-Biogeophys.* **2021**, *126*, e2020JG005942. [[CrossRef](#)]
10. Gherardi, L.A.; Sala, O.E. Effect of interannual precipitation variability on dryland productivity: A global synthesis. *Glob. Chang. Biol.* **2019**, *25*, 269–276. [[CrossRef](#)]
11. Hoover, D.L.; Pfennigwerth, A.A.; Duniway, M.C. Drought resistance and resilience: The role of soil moisture-plant interactions and legacies in a dryland ecosystem. *J. Ecol.* **2021**, *109*, 3280–3294. [[CrossRef](#)]
12. Pettorelli, N.; Laurance, W.F.; O'Brien, T.G.; Wegmann, M.; Nagendra, H.; Turner, W. Satellite remote sensing for applied ecologists: Opportunities and challenges. *J. Appl. Ecol.* **2014**, *51*, 839–848. [[CrossRef](#)]
13. Thomas, C.D.; Cameron, A.; Green, R.E.; Bakkenes, M.; Beaumont, L.J.; Collingham, Y.C.; Erasmus, B.F.; De Siqueira, M.F.; Grainger, A.; Hannah, L.; et al. Extinction risk from climate change. *Nature* **2004**, *427*, 145–148. [[CrossRef](#)] [[PubMed](#)]
14. Seddon, A.W.; Macias-Fauria, M.; Long, P.R.; Benz, D.; Willis, K.J. Sensitivity of global terrestrial ecosystems to climate variability. *Nature* **2016**, *531*, 229–232. [[CrossRef](#)]
15. Li, L.; Zhang, Y.; Wu, J.; Li, S.; Zhang, B.; Zu, J.; Zhang, H.; Ding, M.; Paudel, B. Increasing sensitivity of alpine grasslands to climate variability along an elevational gradient on the Qinghai-Tibet plateau. *Sci. Total Environ.* **2019**, *678*, 21–29. [[CrossRef](#)] [[PubMed](#)]
16. Li, M.; Wu, J.S.; Song, C.Q.; He, Y.T.; Niu, B.; Fu, G.; Tarolli, P.; Tietjen, B.; Zhang, X.Z. Temporal variability of precipitation and biomass of alpine grasslands on the northern tibetan plateau. *Remote Sens.* **2019**, *11*, 360. [[CrossRef](#)]
17. Yao, Y.; Wang, X.; Li, Y.; Wang, T.; Shen, M.; Du, M.; He, H.; Li, Y.; Luo, W.; Ma, M.; et al. Spatiotemporal pattern of gross primary productivity and its covariation with climate in China over the last thirty years. *Glob. Chang. Biol.* **2018**, *24*, 184–196. [[CrossRef](#)]
18. Yuan, Y.; Bao, A.; Liu, T.; Zheng, G.; Jiang, L.; Guo, H.; Jiang, P.; Yu, T.; de Maeyer, P. Assessing vegetation stability to climate variability in central Asia. *J. Environ. Manag.* **2021**, *298*, 113330. [[CrossRef](#)]
19. Henn, J.J.; Buzzard, V.; Enquist, B.J.; Halbritter, A.H.; Klanderud, K.; Maitner, B.S.; Michaletz, S.T.; Potsch, C.; Seltzer, L.; Telford, R.J.; et al. Intraspecific trait variation and phenotypic plasticity mediate alpine plant species response to climate change. *Front. Plant Sci.* **2018**, *9*, 1548. [[CrossRef](#)]
20. Liu, Y.; Men, M.; Peng, Z.; Houx, J.H., 3rd; Peng, Y. Nitrogen availability determines ecosystem productivity in response to climate warming. *Ecology* **2022**, e3823. [[CrossRef](#)]

21. Palmquist, K.A.; Schlaepfer, D.R.; Renne, R.R.; Torbit, S.C.; Doherty, K.E.; Remington, T.E.; Watson, G.; Bradford, J.B.; Lauenroth, W.K. Divergent climate change effects on widespread dryland plant communities driven by climatic and ecohydrological gradients. *Glob. Chang. Biol.* **2021**, *27*, 5169–5185. [[CrossRef](#)]
22. Violle, C.; Navas, M.L.; Vile, D.; Kazakou, E.; Fortunel, C.; Hummel, I.; Garnier, E. Let the concept of trait be functional! *Oikos* **2007**, *116*, 882–892. [[CrossRef](#)]
23. McGill, B.J.; Enquist, B.J.; Weiher, E.; Westoby, M. Rebuilding community ecology from functional traits. *Trends Ecol. Evol.* **2006**, *21*, 178–185. [[CrossRef](#)] [[PubMed](#)]
24. Kearney, M.; Porter, W.P. Ecologists have already started rebuilding community ecology from functional traits. *Trends Ecol. Evol.* **2006**, *21*, 481–482; author reply 482–483. [[CrossRef](#)]
25. Bruelheide, H.; Dengler, J.; Purschke, O.; Lenoir, J.; Jimenez-Alfaro, B.; Hennekens, S.M.; Botta-Dukat, Z.; Chytrý, M.; Field, R.; Jansen, F.; et al. Global trait-environment relationships of plant communities. *Nat. Ecol. Evol.* **2018**, *2*, 1906–1917. [[CrossRef](#)]
26. De Bello, F.; Lepš, J.A.N.; Sebastià, M.-T. Predictive value of plant traits to grazing along a climatic gradient in the Mediterranean. *J. Appl. Ecol.* **2005**, *42*, 824–833. [[CrossRef](#)]
27. Guo, X.; Liu, H.; Ngosong, C.; Li, B.; Wang, Q.; Zhou, W.; Nie, M. Response of plant functional traits to nitrogen enrichment under climate change: A meta-analysis. *Sci. Total Environ.* **2022**, *834*, 155379. [[CrossRef](#)]
28. Midolo, G.; Kuss, P.; Wellstein, C. Land use and water availability drive community-level plant functional diversity of grasslands along a temperature gradient in the Swiss Alps. *Sci. Total Environ.* **2021**, *764*, 142888. [[CrossRef](#)]
29. Prieto, I.; Roumet, C.; Cardinael, R.; Dupraz, C.; Jourdan, C.; Kim, J.H.; Maeght, J.L.; Mao, Z.; Pierret, A.; Portillo, N.; et al. Root functional parameters along a land-use gradient: Evidence of a community-level economics spectrum. *J. Ecol.* **2015**, *103*, 361–373. [[CrossRef](#)]
30. Wang, H.; Wang, R.; Harrison, S.P.; Prentice, I.C. Leaf morphological traits as adaptations to multiple climate gradients. *J. Ecol.* **2022**, *110*, 1344–1355. [[CrossRef](#)]
31. Balachowski, J.A.; Volaire, F.A. Implications of plant functional traits and drought survival strategies for ecological restoration. *J. Appl. Ecol.* **2018**, *55*, 631–640. [[CrossRef](#)]
32. Lian, X.; Piao, S.L.; Chen, A.P.; Huntingford, C.; Fu, B.J.; Li, L.Z.X.; Huang, J.P.; Sheffield, J.; Berg, A.M.; Keenan, T.F.; et al. Multifaceted characteristics of dryland aridity changes in a warming world. *Nat. Rev. Earth Environ.* **2021**, *2*, 232–250. [[CrossRef](#)]
33. Woods, H.A.; Makino, W.; Cotner, J.B.; Hobbie, S.E.; Harrison, J.F.; Acharya, K.; Elser, J.J. Temperature and the chemical composition of poikilothermic organisms. *Funct. Ecol.* **2003**, *17*, 237–245. [[CrossRef](#)]
34. Zhang, Q.; Zhou, J.; Li, X.; Yang, Z.; Zheng, Y.; Wang, J.; Lin, W.; Xie, J.; Chen, Y.; Yang, Y. Are the combined effects of warming and drought on foliar c:N:P:K stoichiometry in a subtropical forest greater than their individual effects? *For. Ecol. Manag.* **2019**, *448*, 256–266. [[CrossRef](#)]
35. Sun, Y.; Liao, J.H.; Zou, X.M.; Xu, X.; Yang, J.Y.; Chen, H.Y.H.; Ruan, H.H. Coherent responses of terrestrial c:N stoichiometry to drought across plants, soil, and microorganisms in forests and grasslands. *Agric. For. Meteorol.* **2020**, *292–293*, 108104. [[CrossRef](#)]
36. Niu, D.; Zhang, C.; Ma, P.; Fu, H.; Elser, J.J. Responses of leaf c:N:P stoichiometry to water supply in the desert shrub *Zygophyllum xanthoxylum*. *Plant Biol.* **2019**, *21*, 82–88. [[CrossRef](#)]
37. Castellanos, A.E.; Llano-Sotelo, J.M.; Machado-Encinas, L.I.; Lopez-Pina, J.E.; Romo-Leon, J.R.; Sardans, J.; Penuelas, J. Foliar c, n, and p stoichiometry characterize successful plant ecological strategies in the Sonoran desert. *Plant Ecol.* **2018**, *219*, 775–788. [[CrossRef](#)]
38. Huang, J.; Wang, P.; Niu, Y.; Yu, H.; Ma, F.; Xiao, G.; Xu, X. Changes in c:N:P stoichiometry modify n and p conservation strategies of a desert steppe species *Glycyrrhiza uralensis*. *Sci. Rep.* **2018**, *8*, 12668. [[CrossRef](#)]
39. Jiang, Y.Y.; Rocha, A.V.; Rastetter, E.B.; Shaver, G.R.; Mishra, U.; Zhuang, Q.L.; Kwiatkowski, B.L. C-n-p interactions control climate driven changes in regional patterns of c storage on the north slope of Alaska. *Landsc. Ecol.* **2016**, *31*, 195–213. [[CrossRef](#)]
40. Delgado-Baquerizo, M.; Maestre, F.T.; Gallardo, A.; Bowker, M.A.; Wallenstein, M.D.; Quero, J.L.; Ochoa, V.; Gozalo, B.; Garcia-Gomez, M.; Soliveres, S.; et al. Decoupling of soil nutrient cycles as a function of aridity in global drylands. *Nature* **2013**, *502*, 672–676. [[CrossRef](#)]
41. Jiao, F.; Shi, X.R.; Han, F.P.; Yuan, Z.Y. Increasing aridity, temperature and soil pH induce soil c-n-p imbalance in grasslands. *Sci. Rep.* **2016**, *6*, 19601. [[CrossRef](#)] [[PubMed](#)]
42. Fiedler, S.; Monteiro, J.A.F.; Hulvey, K.B.; Standish, R.J.; Perring, M.P.; Tietjen, B. Global change shifts trade-offs among ecosystem functions in woodlands restored for multifunctionality. *J. Appl. Ecol.* **2021**, *58*, 1705–1717. [[CrossRef](#)]
43. Jäschke, Y.; Heberling, G.; Wesche, K. Environmental controls override grazing effects on plant functional traits in Tibetan rangelands. *Funct. Ecol.* **2020**, *34*, 747–760. [[CrossRef](#)]
44. Gross, N.; Bagousse-Pinguet, Y.L.; Liancourt, P.; Berdugo, M.; Gotelli, N.J.; Maestre, F.T. Functional trait diversity maximizes ecosystem multifunctionality. *Nat. Ecol. Evol.* **2017**, *1*, 132. [[CrossRef](#)] [[PubMed](#)]
45. He, N.; Li, Y.; Liu, C.; Xu, L.; Li, M.; Zhang, J.; He, J.; Tang, Z.; Han, X.; Ye, Q.; et al. Plant trait networks: Improved resolution of the dimensionality of adaptation. *Trends Ecol. Evol.* **2020**, *35*, 908–918. [[CrossRef](#)] [[PubMed](#)]
46. He, N.; Liu, C.; Piao, S.; Sack, L.; Xu, L.; Luo, Y.; He, J.; Han, X.; Zhou, G.; Zhou, X.; et al. Ecosystem traits linking functional traits to macroecology. *Trends Ecol. Evol.* **2019**, *34*, 200–210. [[CrossRef](#)]
47. Jin, X.M.; Liu, J.T.; Wang, S.T.; Xia, W. Vegetation dynamics and their response to groundwater and climate variables in Qaidam basin, China. *Int. J. Remote Sens.* **2016**, *37*, 710–728. [[CrossRef](#)]

48. Han, J.J.; Wang, J.P.; Chen, L.; Xiang, J.Y.; Ling, Z.Y.; Li, Q.K.; Wang, E.L. Driving factors of desertification in Qaidam basin, China: An 18-year analysis using the geographic detector model. *Ecol. Indic.* **2021**, *124*, 107404. [CrossRef]
49. Shi, X.; Yu, D.; Warner, E.; Pan, X.; Petersen, G.; Gong, Z.; Weindorf, D. Soil database of 1:1,000,000 digital soil survey and reference system of the Chinese genetic soil classification system. *Soil Surv. Horiz.* **2004**, *45*, 129–136. [CrossRef]
50. Zhang, S.Q.; Chen, H.; Fu, Y.; Niu, H.H.; Yang, Y.; Zhang, B.X. Fractional vegetation cover estimation of different vegetation types in the Qaidam basin. *Sustainability* **2019**, *11*, 864. [CrossRef]
51. Fu, Y.; Chen, H.; Niu, H.H.; Zhang, S.Q.; Yang, Y. Spatial and temporal variation of vegetation phenology and its response to climate changes in Qaidam basin from 2000 to 2015. *J. Geogr. Sci.* **2018**, *28*, 400–414. [CrossRef]
52. Savitzky, A.; Golay, M.J. Smoothing and differentiation of data by simplified least squares procedures. *Anal. Chem.* **1964**, *36*, 1627–1639. [CrossRef]
53. Holben, B.N. Characteristics of maximum-value composite images from temporal AVHRR data. *Int. J. Remote Sens.* **1986**, *7*, 1417–1434. [CrossRef]
54. Hutchinson, M. *ANUSPLIN*, version 4.3; Centre for Resource and Environmental Studies, The Australian National University: Canberra, Australia, 2004.
55. Li, M.; Wu, J.S.; He, Y.T.; Wu, L.; Niu, B.; Song, M.H.; Zhang, X.Z. Dimensionality of grassland stability shifts along with altitudes on the Tibetan plateau. *Agric. For. Meteorol.* **2020**, *291*, 108080. [CrossRef]
56. Sandholt, I.; Rasmussen, K.; Andersen, J. A simple interpretation of the surface temperature/vegetation index space for assessment of surface moisture status. *Remote Sens. Environ.* **2002**, *79*, 213–224. [CrossRef]
57. Kendall, M.G. *Rank Correlation Methods*, 4th ed.; Charles Griffin: London, UK, 1975.
58. Mann, H.B. Nonparametric tests against trend. *Econometrica* **1945**, *13*, 245–259. [CrossRef]
59. Akhtar, K.; Wang, W.Y.; Ren, G.X.; Khan, A.; Feng, Y.Z.; Yang, G.H. Changes in soil enzymes, soil properties, and maize crop productivity under wheat straw mulching in Guanzhong, China. *Soil Till. Res.* **2018**, *182*, 94–102. [CrossRef]
60. Wu, J.S.; Song, M.H.; Ma, W.L.; Zhang, X.Z.; Shen, Z.X.; Tarolli, P.; Wurst, S.; Shi, P.L.; Ratzmann, G.; Feng, Y.F.; et al. Plant and soil's  $\delta^{15}N$  are regulated by climate, soil nutrients, and species diversity in alpine grasslands on the northern Tibetan plateau. *Agric. Ecosyst. Environ.* **2019**, *281*, 111–123. [CrossRef]
61. Gauzere, P.; Doucier, G.; Devictor, V.; Kefi, S. A framework for estimating species-specific contributions to community indicators. *Ecol. Indic.* **2019**, *99*, 74–82. [CrossRef]
62. Violle, C.; Reich, P.B.; Pacala, S.W.; Enquist, B.J.; Kattge, J. The emergence and promise of functional biogeography. *Proc. Natl. Acad. Sci. USA* **2014**, *111*, 13690–13696. [CrossRef]
63. Wilcoxon, F. Individual comparisons by ranking methods. In *Breakthroughs in Statistics*; Springer: Berlin/Heidelberg, Germany, 1992; pp. 196–202.
64. Wei, T.; Simko, V. R Package “Corrplot”: Visualization of a Correlation Matrix (Version 0.92). 2021. Available online: <https://github.com/taiyun/corrplot> (accessed on 26 February 2022).
65. Niu, W.; Chen, H.; Wu, J. Soil moisture and soluble salt content dominate changes in foliar  $\delta^{13}C$  and  $\delta^{15}N$  of desert communities in the Qaidam basin, Qinghai-Tibetan plateau. *Front. Plant Sci.* **2021**, *12*, 675817. [CrossRef]
66. Wu, J.; Li, M.; Fiedler, S.; Ma, W.; Wang, X.; Zhang, X.; Tietjen, B. Impacts of grazing exclusion on productivity partitioning along regional plant diversity and climatic gradients in Tibetan alpine grasslands. *J. Environ. Manag.* **2019**, *231*, 635–645. [CrossRef]
67. Rosseel, Y. Lavaan: An R package for structural equation modeling. *J. Stat. Softw.* **2012**, *48*, 1–36. [CrossRef]
68. R Core Team. *R: A Language and Environment for Statistical Computing*; R Foundation for Statistical Computing: Vienna, Austria, 2021.
69. ESRI. *ArcGIS Desktop: Release 10.2*; Environmental Systems Research Institute: Redlands, CA, USA, 2014.
70. Kusch, E.; Davy, R.; Seddon, A.W.R. Vegetation-memory effects and their association with vegetation resilience in global drylands. *J. Ecol.* **2022**, *110*, 1561–1574. [CrossRef]
71. Ogle, K.; Barber, J.J.; Barron-Gafford, G.A.; Bentley, L.P.; Young, J.M.; Huxman, T.E.; Loik, M.E.; Tissue, D.T. Quantifying ecological memory in plant and ecosystem processes. *Ecol. Lett.* **2015**, *18*, 221–235. [CrossRef] [PubMed]
72. Easterling, D.R.; Wehner, M.F. Is the climate warming or cooling? *Geophys. Res. Lett.* **2009**, *36*. [CrossRef]
73. Zhu, Y.K.; Zhang, J.T.; Zhang, Y.Q.; Qin, S.G.; Shao, Y.Y.; Gao, Y. Responses of vegetation to climatic variations in the desert region of northern China. *Catena* **2019**, *175*, 27–36. [CrossRef]
74. Olson, M.E.; Soriano, D.; Rosell, J.A.; Anfodillo, T.; Donoghue, M.J.; Edwards, E.J.; Leon-Gomez, C.; Dawson, T.; Camarero Martinez, J.J.; Castorena, M.; et al. Plant height and hydraulic vulnerability to drought and cold. *Proc. Natl. Acad. Sci. USA* **2018**, *115*, 7551–7556. [CrossRef]
75. Kraft, N.J.B.; Adler, P.B.; Godoy, O.; James, E.C.; Fuller, S.; Levine, J.M. Community assembly, coexistence and the environmental filtering metaphor. *Funct. Ecol.* **2015**, *29*, 592–599. [CrossRef]
76. Aerts, R.; Chapin, F.S. The mineral nutrition of wild plants revisited: A re-evaluation of processes and patterns. In *Advances in Ecological Research*; Fitter, A.H., Raffaelli, D.G., Eds.; Academic Press: Cambridge, MA, USA, 2000; Volume 30, pp. 1–67.
77. Hobbie, S.E.; Nadelhoffer, K.J.; Hogberg, P. A synthesis: The role of nutrients as constraints on carbon balances in boreal and arctic regions. *Plant Soil* **2002**, *242*, 163–170. [CrossRef]
78. Kirschbaum, M.U.F. The temperature-dependence of soil organic-matter decomposition, and the effect of global warming on soil organic-c storage. *Soil Biol. Biochem.* **1995**, *27*, 753–760. [CrossRef]

79. Sparks, D.L.; Liebhardt, W.C. Temperature effects on potassium exchange and selectivity in Delaware soils. *Soil Sci.* **1982**, *133*, 10–17. [[CrossRef](#)]
80. Lewis, J.D.; Lucash, M.; Olszyk, D.M.; Tingey, D.T. Relationships between needle nitrogen concentration and photosynthetic responses of douglas-fir seedlings to elevated CO<sub>2</sub> and temperature. *New Phytol.* **2004**, *162*, 355–364. [[CrossRef](#)]
81. Berry, J.; Bjorkman, O. Photosynthetic response and adaptation to temperature in higher plants. *Annu. Rev. Plant Physiol.* **1980**, *31*, 491–543. [[CrossRef](#)]
82. Field, C. The photosynthesis-nitrogen relationship in wild plants. In *On the Economy of Form and Function*; Cambridge University Press: Cambridge, UK, 1986.
83. Wright, I.J.; Reich, P.B.; Westoby, M. Strategy shifts in leaf physiology, structure and nutrient content between species of high- and low-rainfall and high- and low-nutrient habitats. *Funct. Ecol.* **2001**, *15*, 423–434. [[CrossRef](#)]
84. Wright, I.J.; Reich, P.B.; Cornelissen, J.H.; Falster, D.S.; Garnier, E.; Hikosaka, K.; Lamont, B.B.; Lee, W.; Oleksyn, J.; Osada, N.; et al. Assessing the generality of global leaf trait relationships. *New Phytol.* **2005**, *166*, 485–496. [[CrossRef](#)]
85. Blackwell, M.S.A.; Brookes, R.C.; de la Fuente-Martinez, N.; Gordon, H.; Murray, P.J.; Snars, K.E.; Williams, J.K.; Bol, R.; Haygarth, P.M. Chapter 1—Phosphorus solubilization and potential transfer to surface waters from the soil microbial biomass following drying–rewetting and freezing–thawing. In *Advances in Agronomy*; Sparks, D.L., Ed.; Elsevier: Amsterdam, The Netherlands, 2010; Volume 106, pp. 1–35.
86. Wang, R.Z.; Creamer, C.A.; Wang, X.; He, P.; Xu, Z.W.; Jiang, Y. The effects of a 9-year nitrogen and water addition on soil aggregate phosphorus and sulfur availability in a semi-arid grassland. *Ecol. Indic.* **2016**, *61*, 806–814. [[CrossRef](#)]
87. Farooqui, A.; Pillai, S.K.; Agnihotri, D.; Khan, S.; Tewari, R.; Shukla, S.K.; Ali, S.; Trivedi, A.; Pandita, S.K.; Kumar, K.; et al. Impact of climate on the evolution of vegetation in tectonically active Karewa basin, Kashmir Himalayas. *J. Earth Syst. Sci.* **2021**, *130*, 93. [[CrossRef](#)]
88. Li, Z.; Tian, D.; Wang, B.; Wang, J.; Wang, S.; Chen, H.Y.H.; Xu, X.; Wang, C.; He, N.; Niu, S. Microbes drive global soil nitrogen mineralization and availability. *Glob. Chang. Biol.* **2019**, *25*, 1078–1088. [[CrossRef](#)] [[PubMed](#)]
89. Trenberth, K.E.; Dai, A.G.; van der Schrier, G.; Jones, P.D.; Barichivich, J.; Briffa, K.R.; Sheffield, J. Global warming and changes in drought. *Nat. Clim. Chang.* **2014**, *4*, 17–22. [[CrossRef](#)]
90. Brenner, D.L.; Amundson, R.; Baisden, W.T.; Kendall, C.; Harden, J. Soil n and n-15 variation with time in a California annual grassland ecosystem. *Geochim. Cosmochim. Acta* **2001**, *65*, 4171–4186. [[CrossRef](#)]
91. Evans, S.E.; Burke, I.C. Carbon and Nitrogen Decoupling Under an 11-Year Drought in the Shortgrass Steppe. *Ecosystems* **2013**, *16*, 704–705. [[CrossRef](#)]
92. Körner, C.; Körner, C. *Alpine Plant Life: Functional Plant Ecology of High Mountain Ecosystems*; Springer: Berlin/Heidelberg, Germany, 1999.
93. Kuchenbuch, R.; Claassen, N.; Jungk, A. Potassium availability in relation to soil moisture. *Plant Soil* **1986**, *95*, 233–243. [[CrossRef](#)]
94. Bargagli, R.; Brown, D.H.; Nelli, L. Metal biomonitoring with mosses: Procedures for correcting for soil contamination. *Environ. Pollut.* **1995**, *89*, 169–175. [[CrossRef](#)]
95. Mahlstein, I.; Daniel, J.S.; Solomon, S. Pace of shifts in climate regions increases with global temperature. *Nat. Clim. Chang.* **2013**, *3*, 739–743. [[CrossRef](#)]
96. Moles, A.T.; Perkins, S.E.; Laffan, S.W.; Flores-Moreno, H.; Awasthy, M.; Tindall, M.L.; Sack, L.; Pitman, A.; Kattge, J.; Aarssen, L.W.; et al. Which is a better predictor of plant traits: Temperature or precipitation? *J. Veg. Sci.* **2014**, *25*, 1167–1180. [[CrossRef](#)]
97. Coban, O.; de Deyn, G.B.; van der Ploeg, M. Soil microbiota as game-changers in restoration of degraded lands. *Science* **2022**, *375*, abe0725. [[CrossRef](#)]
98. Watanabe, T.; Broadley, M.R.; Jansen, S.; White, P.J.; Takada, J.; Satake, K.; Takamatsu, T.; Tuah, S.J.; Osaki, M. Evolutionary control of leaf element composition in plants. *New Phytol.* **2007**, *174*, 516–523. [[CrossRef](#)]